AERODYNAMICS OF END-WALL BOUNDARY LAYER IN A VORTEX CHAMBER

É. P. Volchkov, S. V. Semenov, and V. I. Terekhov

UDC 532.59.001.572

The need for the inclusion of end-wall boundary layers in the study of the aerodynamics of vortex chambers has been frequently mentioned in the literature. However, owing to limited experimental data [1-3] with reliable information on the wall layers, the existing computational methods for end-wall boundary layers are not well-founded. The question of which parameters determine the formation of end-wall flow remains debatable. In some studies [4, 5], the vortex chambers are conditionally divided into short and long chambers. However, there is no unique opinion on the role of end-wall flows in vortex chambers of different lengths. It has also not been established for what geometric and flow parameters the chamber could be considered long or short. In the present study, as in [1, 5-8], solution is obtained for the end-wall boundary-layer equations using integral methods, considering the boundary layer in the radial direction in the form of a submerged wall jet. Such an approach made it possible to use the laws for the development of wall jets [9], and obtain fairly simple relations for integral parameters, skin friction, mass flow in the boundary layer, and other characteristics. Results are compared with available experimental data and computations of others authors; turbulent flow is considered; results for laminar boundary layer are given in [10].

1. Problem Formulation. Derivation of Momentum Integral Relation for End-Wall Boundary Layer

The first theoretical studies [6, 7] considered the interaction of rotational flow with end-walls in vortex chambers. It was assumed that the end-wall boundary layer, as it develops along the radius of the chamber, can be split into two regions (Fig. 1): I ($\bar{r}^* \le r \le 1$), the developing region, and II ($r_0 \le r \le r^*$), the developed region. Here, $\bar{r}^* = r^*/R_k$ is the radius enclosing region II, where the entire gas Q_k passes through the end-wall boundary layers and the radial velocity component in the region outside the boundary layers is equal to zero. It was also assumed in [4, 6-8] that the flow in the core of vortex chamber is inviscid while in the region I the rotation of the gas takes place with constant circulation $\Gamma_0 = v_0 r = v_k R_k = \text{const}$. In region II, the radial velocity component in the core of the flow $u_0 = 0$ and the circulation toward the center of the chamber decreases such that it satisfies the condition $2Q_T = Q_K$, $2Q_T$ being the total volume flow of gas through the upper and lower ends of the chamber. Finally, the problem is reduced to the determination of the quantity $\bar{r}^*$ and the variation of circulation in region II. Following [4, 6, 8], we use the flow pattern shown in Fig. 1. The available experimental data [11, 12] show that the general picture of the flow in regions I and II is maintained with changes in the radius of the outlet hole r_0. Region IV, determined by the value of the radius r_0, is undoubtedly important to describe the complete aerodynamic picture in the chamber, but it is not considered in the present study.

Consider boundary layers III that develop symmetrically on the lower and upper end walls of the chamber. Using the usual simplifications, we write the equation of motion and continuity for the end-wall boundary layer in cylindrical coordinates [13]:

$$u\frac{\partial u}{\partial r} + w\frac{\partial u}{\partial z} - \frac{v^2}{r} = -\frac{1}{\rho}\frac{\partial p}{\partial r} + \frac{1}{\rho}\frac{\partial \tau_{rz}}{\partial z},$$
$$u\frac{\partial v}{\partial r} + w\frac{\partial v}{\partial z} + \frac{uv}{r} = \frac{1}{\rho}\frac{\partial \tau_{\varphi z}}{\partial z}, \qquad (1.1)$$
$$\partial p/\partial z = 0, \quad \partial u/\partial r + u/r + \partial w/\partial z = 0.$$

Novosibirsk. Translated from Zhurnal Prikladnoi Mekhaniki i Tekhnicheskoi Fiziki, No. 5, pp. 117-126, September-October, 1986. Original article submitted June 25, 1985.

 0021-8944/86/2705-0740$12.50

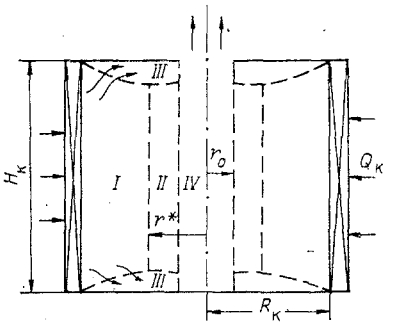

Fig. 1

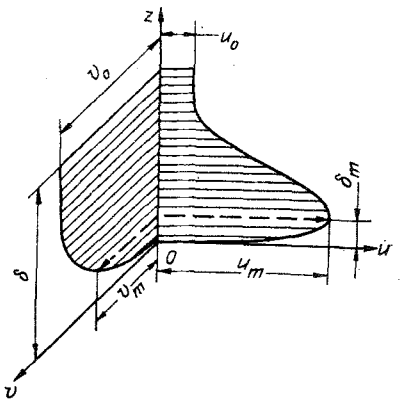

Fig. 2

Here τ is the shear stress tensor, equal to the sum of viscous and turbulent (eddy) components; u, v, and w are the radial, tangential, and axial velocity components.

In the inviscid regions I and II, Navier–Stokes equations give

$$u_0 \frac{\partial u_0}{\partial r} - \frac{v_0^2}{r} = -\frac{1}{\rho}\frac{\partial p}{\partial r}, \tag{1.2}$$

$$u_0 \partial v_0/\partial r + u_0 v_0/r = 0, \quad \partial p/\partial z = 0, \quad \partial u_0/\partial r + u_0/r + \partial w_0/\partial z = 0.$$

Here it was assumed that the radial u_0 and circumferential v_0 velocity components in these regions do not change with the height of the chamber. The index 0 in Eq. (1.2) denotes parameters outside the end-wall boundary layer. The second equation of system (1.2) is expressed in the form

$$\frac{1}{r} u_0 \frac{\partial \Gamma_0}{\partial r} = 0,$$

to obtain $\Gamma_0 = \Gamma_k = v_k R_k = \text{const}$ for $u_0 \neq 0$, i.e., the circulation of the flow outside the end-wall layer in the region I ($\bar{r}^* < r < 1$) is potential (Γ_k is the circulation at the chamber inlet).

Actually, the manifestation of viscosity in the rotating flow in the region outside the boundary layers takes place with a loss in circulation:

$$\frac{v_0}{v_k}\frac{r^m}{R_k^m} = \bar{v}_0 \bar{r}^m = 1, \tag{1.3}$$

where v_k is the circumferential velocity at the periphery of the chamber $r = R_k$; $m < 1$. This fact is confirmed by experimental results from tangential flow field measurements in vortex chambers [1, 2, 12]. In particular, in [1, 2] it has been established that, depending on tangential Reynolds number at the periphery $Re_k = v_k R_k/\nu$, the values of m vary within the range 0.65-0.85, where the lower value of m and larger loss of circulation in the chamber correspond to large values of Re_k.

As shown by experiments [1-3], the boundary layer in the tangential direction is a typical shear layer of thickness δ (Fig. 2). The velocity profile of radial flow in the end-wall boundary layer is similar to the velocity distribution in the wall jet. The influence of wall on radial velocity profile is felt on the layer of thickness δ_m in which the radial velocity increases from zero to the maximum value u_m.

Integrating the first equation of the system (1.1) across the thickness of radial wall layer δ_m using the continuity equation for the impermeable and irrotational end wall and with boundary conditions $z = 0$: $u = v = w = 0$, $\tau_{rz} = (\tau_{rz})_w$; $z = \delta_m$: $u = u_m$, $\tau_{rz} = 0$, and after transformations we get momentum integral relations in the radial direction:

$$\frac{1}{\bar{r}}\frac{d\left(\mathrm{Re}_r^{**}\bar{r}\right)}{d\bar{r}} + \frac{1}{u_m}\frac{du_m}{d\bar{r}}\left(1 + \frac{\delta^*}{\delta_r^{**}} + \frac{\delta_m}{\delta_r^{**}}\right) - \mathrm{Re}_r \frac{1}{2}\frac{v_0^2}{u_m^2}\frac{\int_0^{\delta_m}(1-\bar{v}^2)\,dz}{\int_0^{\delta_m}\bar{u}(1-\bar{u})\,dz} = \frac{c_{fr}}{2}\mathrm{Re}_m. \tag{1.4}$$

Here $\bar{u} = u/u_m$, $\bar{v} = v/v_0$ are nondimensional profiles of radial and tangential velocity components in the boundary layer:

$$\mathrm{Re}_r^{**} = u_m\delta_r^{**}/\nu; \quad \delta_r^{**} = \int_0^{\delta_m} \bar{u}(1-\bar{u})\,dz; \quad \delta_r^{*} = \int_0^{\delta_m} (1-\bar{u})\,dz;$$

$$c_{fr}/2 = (\tau_{rz})_w/\rho u_m^2; \quad \mathrm{Re}_m = u_m R_k/\nu.$$

Thus, Eq. (1.4) coincides with similar expressions for wall jets [9]. The exception consists of the third term on the left-hand side of Eq. (1.4) due to the effects of centrifugal forces on the momentum transfer in the radial direction. The integral equations for the tangential direction can be similarly obtained. Finally, integrating the second equation of the system (1.1) across the entire boundary-layer thickness δ [with boundary conditions $z = 0$: $u = v = w = 0$, $\tau_{\varphi z} = (\tau_{\varphi z})_w$; $z = \delta$: $u = w = 0$, $v = v_0$, $\tau_{\varphi z} = 0$],

$$\frac{1}{\bar{r}}\frac{(d\,\mathrm{Re}_\varphi^{**}\bar{r})}{d\bar{r}} - \mathrm{Re}_\varphi^{**}\left(\frac{1}{\bar{r}} + \frac{1}{\bar{v}_0}\frac{\partial \bar{v}_0}{\partial \bar{r}}\right)\overline{W} = \frac{c_{f\varphi}}{2}\mathrm{Re}_m, \tag{1.5}$$

where

$$\bar{v}_0 = v_0/v_k; \quad \overline{W} = \left(\int_0^{\delta} \bar{u}\bar{v}\,dz\right)\Big/\delta_\varphi^{**};$$

$$\mathrm{Re}_\varphi^{**} = u_m\delta_\varphi^{**}/\nu; \quad \delta_\varphi^{**} = \int_0^{\delta} \bar{u}(1-\bar{v})\,dz; \quad c_{f\varphi}/2 = (\tau_{\varphi z})_w/\rho v_0 u_m.$$

The Reynolds number in (1.5) is based on the radial velocity u_m, which is the critical parameter in the momentum transfer process in the boundary layer. The integral quantity δ_φ^{**} is the momentum thickness. In the particular case of irrotational motion of the fluid in the region outside the end wall layer ($m = 1$) on the stationary surface the second term in (1.5) is equal to zero and the equation is considerably simplified.

Obviously, Eqs. (1.4) and (1.5) are applicable for laminar as well as turbulent flows. In order to solve them, it is necessary to know the circumferential and radial velocity profiles across the end-wall layer, the distribution of maximum velocity across the chamber radius $u_m = f(\bar{r})$, and also the skin-friction laws coupling skin-friction coefficients with the integral parameters of the boundary layer. However, the computation is significantly simplified by assuming the ratio of boundary-layer thicknesses to be a constant ($\bar{\delta}_m = \delta_m/\delta$ = const) across the radius of the end-wall surface. Such an approach is widely used in the analysis of wall jets [9, 14, 15]. As shown below, the computed results are weakly dependent on the ratio of boundary-layer thicknesses when it varies within wide limits δ_m/δ = 0.05-0.3. Then Eqs. (1.4) and (1.5) can be solved independent of each other. Since the primary objective is to determine the boundary-layer thickness and mass flow through it, greater attention in this paper is devoted to the solution of the integral relation (1.5).

2. Velocity Distribution in the End-Wall Boundary Layer of the Vortex Chamber

In the majority of studies on turbulent rotating boundary layers the circumferential velocity profile is described by the usual power law

$$v/v_0 = \bar{v} = (z/\delta)^n, \; n = 1/7. \tag{2.1}$$

It was shown in [10] that such power-law approximation is valid only for sufficiently high Reynolds numbers ($\mathrm{Re}_k > 10^5$). Analysis of experimental results showed that $\mathrm{Re}_k > 10^5$ corresponds to fully developed turbulent flow in the end-wall boundary layer.

In order to describe the radial velocity profile, the effective approach, in our view, could be the one used in the analysis of semibounded jet [9, 14]. The boundary layer is divided into two regions: the wall layer $0 < z < \delta_m$ (see Fig. 2) with power laws for wall turbulence $u/u_m = (z/\delta_m)^n$ and the jet region $\delta_m < z < \delta$ where jet-mixing processes predominate. The velocity profile in the jet region is described by the Schlichting equation [15]

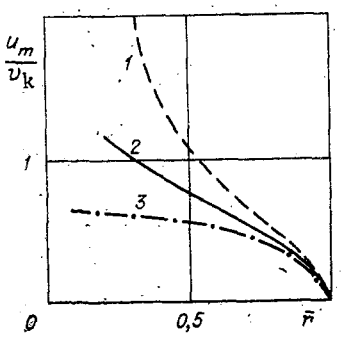

Fig. 3

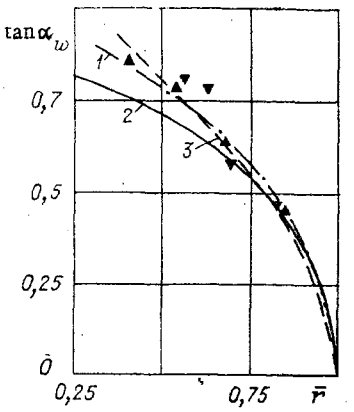

Fig. 4

$$\frac{u-u_0}{u_m-u_0}=\left[1-\left(\frac{z-\delta_m}{\delta-\delta_m}\right)^{1,5}\right]^2. \tag{2.2}$$

Such an approach, as shown by a comparison, gives good agreement with experiment for different cases of interaction of the jet with surfaces [9, 10].

The resultant velocity and its direction in the end-wall layer is found from the circumferential and radial velocity profiles in the form (2.1) and (2.2), assuming

$$V_\Sigma=\sqrt{u^2+v^2},\ \alpha=\operatorname{arctg} u/v,$$

where α is the angle between the resultant velocity and the circumferential direction. In the wall region the boundary layer ($z < \delta_m$) its value is a constant across the thickness and equals the angle of rotation on the wall

$$\operatorname{tg}\alpha=\operatorname{tg}\alpha_w=\frac{u_m}{v_0}\frac{\bar{u}}{\bar{v}}=\frac{u_m}{v_0}\bar{\delta}_m^{-n}.$$

The quantity $\bar{\delta}_m^{-n} = (\delta_m/\delta)^{-n}$ is practically constant in the interval $\delta_m/\delta = 0.05$-0.3; hence,

$$\operatorname{tg}\alpha_w=1{,}4u_m/v_0. \tag{2.3}$$

Consider now the distribution of the maximum value of radial velocity component across the radius of the end wall. This dependence is determined from the system of equations (1.4) and (1.5), and is the parameter sought in the solution of boundary-layer equations [1, 4-8]. However, if the method similar to that suggested for the computation of the maximum velocity in the wall jets [9, 14] is used, it is possible to obtain a fairly simple relation for u_m. The equation of motion in the radial direction is written for $z = \delta_m$ with an initial approximation $(\partial\tau_{rz}/\partial z)_{z=\delta_m} \to 0$. Then it follows from (1.1):

$$u_m\frac{\partial u_m}{\partial r}-\frac{v_m^2}{r}=-\frac{1}{\rho}\frac{\partial p}{\partial r}=u_0\frac{\partial u_0}{\partial r}-\frac{v_0^2}{r}, \tag{2.4}$$

where v_m is the circumferential velocity at the point $z = \delta_m$. Since $u_0 \ll u_m$, the term $u_0\partial u_0/\partial r$ in Eq. (2.4) is neglected.

The integration of (2.4) using (1.3) and the boundary condition $u_m = u_k$ at $r = R_k$, gives

$$u_m/v_k=\left[(u_k/v_k)^2+\left(1-\bar{\delta}_m^{2n}\right)\left(\bar{r}^{-2m}-1\right)/m\right]^{1/2}. \tag{2.5}$$

In the region $\bar{\delta}_m = 0.05$-0.3, the quantity $(1 - \bar{\delta}_m{}^{2n}) \approx 0.4$. Then,

$$u_m/v_k=\left[(u_k/v_k)^2+0{,}4(\bar{r}^{-2m}-1)/m\right]^{1/2}. \tag{2.6}$$

It is worth noting that Eq. (2.6) gives results close to those obtained from numerical solution of Eqs. (1.4) and (1.5).

For the flow in the vortex chamber with intense vortex rollup $u_k \ll v_k$, from (2.6),

$$u_m/v_\kappa = \sqrt{0{,}4\,(\bar{r}^{-2m}-1)/m} \text{ when } m \neq 0,\ u_m/v_\kappa = \sqrt{0{,}8\ln(1/\bar{r})} \text{ when } m = 0. \tag{2.7}$$

The variation of the maximum value of the radial velocity component along the radius of the chamber in the end-wall boundary layer and computed from Eq. (2.7) is shown in Fig. 3. Characteristically, the distribution of tangential velocity component outside the boundary layers strongly affects the development of radial flow. It is seen from Fig. 3 that the strongest radial flow in the neighborhood of end walls occurs with the rotation of the fluid from the conservation of circulation (curve 1); constant velocity flow is reflected by curve 2, and curve 3 describes the flow with constant angular velocity.

The variation of the angle of flow rollup at the wall for the motion along the radius of the end wall is found from Eqs. (2.3) and (2.7):

$$\operatorname{tg}\alpha_w = \bar{\delta}_m^{-n}\bar{r}^{-m}\left[0{,}4\,(\bar{r}^{-2m}-1)/m\right]^{1/2} \text{ when } m \neq 0; \tag{2.8}$$

$$\operatorname{tg}\alpha_w = \bar{\delta}_m^{-n}\left[0{,}8\ln(1/\bar{r})\right]^{1/2} \text{ when } m = 0; \tag{2.9}$$

$$\operatorname{tg}\alpha_w = 0{,}83\sqrt{1-\bar{r}^2} \text{ when } m = 1. \tag{2.10}$$

Experimental values of the rollup of the flow at the end wall of the vortex chamber [1, 2] practically coincide with computed results from Eq. (2.8) for the mean experimental value of m = 0.7 (Fig. 4, line 1). Here, for the purposes of comparison, the line 2 denotes computation from Eq. (2.10) for the flow with constant circulation (m = 1). The results of numerical solution [8] (curve 3) appear to be sufficiently close to the experimental and the present computed data. It is seen that the angle of the flow rollup sharply increases during the motion from the periphery of the chamber to the center, which is caused by an increase in radial flow along the end wall toward the center.

3. Skin-Friction Laws for Three-Dimensional Turbulent Boundary Layer

Prandtl's hypothesis for three-dimensional turbulent boundary layer is used to derive the skin-friction laws. The expression for turbulent skin friction has the form

$$\tau_\Sigma = \sqrt{\tau_{\varphi z}^2 + \tau_{rz}^2} = \rho l^2 (\partial V_\Sigma/\partial z)^2, \tag{3.1}$$

where $V_\Sigma = \sqrt{v^2 + u^2}$ is the resultant velocity in the wall region of the boundary layer. The angle of flow rollup does not change across the wall-region thickness $0 < z < \delta_m$, and hence the direction of the resultant velocity and the shear stress here coincide. Then

$$\tau_{\varphi z} = \tau_\Sigma \cos\alpha_w,\ \tau_{rz} = \tau_\Sigma \sin\alpha_w. \tag{3.2}$$

Assuming that the skin-friction law for the total shear stress in the three-dimensional boundary layer is the same as that on a flat plate [14],

$$(\tau_\Sigma)_w/\rho V_{\Sigma_m}^2 = B/2\left(\mathrm{Re}_{\Sigma_m}^{**}\right)^{-1/4}, \tag{3.3}$$

where for $\mathrm{Re}_{\Sigma m}^{**} < 10^4$, B/2 = 0.0128. Here it is necessary to remember that the characteristic speed in (3.3) is the resultant velocity at the edge of the wall layer ($z = \delta_m$)

$$V_{\Sigma_m} = \sqrt{u_m^2 + v_m^2} = \bar{\delta}_m^n v_0 \sqrt{1 + \operatorname{tg}^2\alpha_w}. \tag{3.4}$$

The Reynolds number (3.3) is also similarly based on this velocity:

$$\mathrm{Re}_{\Sigma_m}^{**} = V_{\Sigma_m}\delta_{\Sigma_m}^{**}/\nu,\quad \delta_{\Sigma_m}^{**} = \int_0^{\delta_m} V_\Sigma/V_{\Sigma_m}\left(1 - V_\Sigma/V_{\Sigma_m}\right)dz.$$

Equations (3.2) and (3.3) are used to find expressions for skin friction at the wall in the tangential direction

$$c_{f\varphi}/2 = (\tau_{\varphi z})_w/\rho u_m v_0 = B/2\left(\mathrm{Re}_\varphi^{**}\right)^{-1/4}\bar{\delta}_m^{n-1/4}\left[(1 + \operatorname{tg}^2\alpha_w)/\operatorname{tg}^2\alpha_w\right]^{3/8} \tag{3.5}$$

TABLE 1

$\bar{\delta}_m$	$\delta_\varphi^{**}/\delta$	c	$\bar{W}$	$\bar{\delta}_m$	$\delta_\varphi^{**}/\delta$	c	$\bar{W}$
0,05	0,092	5,147	4,150	0,2	0,095	5,620	4,618
0,1	0,093	5,302	4,305	0,25	0,096	5,779	4,780
0,15	0,094	5,465	4,46	0,3	0,097	5,942	4,947

and the radial direction

$$c_{fr}/2 = (\tau_{rz})_w/\rho u_m^2 = B/2\,(\mathrm{Re}_r^{**})^{-1/4}\,[(1+\mathrm{tg}^2\alpha_w)/\mathrm{tg}^2\alpha_w]^{3/8}. \tag{3.6}$$

Thus, the relations obtained for the maximum value of the radial velocity component (2.7), the angle of rollup at the wall (2.8)-(2.10), and skin-friction laws (3.5) and (3.6) make it possible to solve the integral equations (1.4) and (1.5) for the developing flow region.

4. Solution of Momentum Integral Relations. Discussion of Results

Using the skin-friction law in the form (3.5) and the velocity distribution outside the end-wall layer (1.3), Eq. (1.5) is expressed in the form

$$\frac{d\,\mathrm{Re}_\varphi^{**}}{d\bar{r}} + \frac{\mathrm{Re}_\varphi^{**}}{\bar{r}}\,[1-\bar{W}(1-m)] = \\ = -\frac{B}{2}(\mathrm{Re}_\varphi^{**})^{-1/4}\,\bar{\delta}_m^{2n-1/4}\,\mathrm{tg}^{1/4}\alpha_w\,(1+\mathrm{tg}^2\alpha_w)^{3/8}\,\bar{r}^{-m}\,\mathrm{Re}_{k*} \tag{4.1}$$

Here $\mathrm{Re}_k = v_k R_k/\nu$ is the tangential Reynolds number at the periphery of the chamber.

Initially computations were made relative to the momentum thickness $\delta\varphi^{**}/\delta$, integral parameter $\bar{W}$, and the parameter $C = \left(\int_0^\delta u dz\right)\Big/\delta_\varphi^{**}$, characterizing the mass flow through the end-wall layer. Computational results in the interval $\bar{\delta}_m$ = 0.05-0.3, including the range of experimental values, are given in the table. The weak dependence of integral parameters on δ_m considerably simplifies further analysis. Hence, as mentioned above, Eq. (4.1) can be solved independently of the momentum integral relations in the radial direction (1.4).

The expression for the angle of rollup of the flow at the wall (2.8) is used to write Eq. (4.1) as

$$\frac{d\,\mathrm{Re}_\varphi^{**}}{d\bar{r}} + \frac{\mathrm{Re}_\varphi^{**}}{\bar{r}}\,[1-\bar{W}(1-m)] = \\ = -\frac{B}{2}(\mathrm{Re}_\varphi^{**})^{-1/4}\,\bar{\delta}_m^{2n-1/4}\,(\bar{\delta}_m^{-2n}-1)^{1/8}\,\bar{r}^{-(m+1/4)}\,\mathrm{Re}_k M(\bar{r}), \tag{4.2}$$

where

$$M(\bar{r}) = \left\{\left[1+\frac{1-\bar{\delta}_m^{2n}}{m\bar{\delta}_m^{2n}}(1-\bar{r}^{2m})\right]^3 \bar{r}^2\,(1-\bar{r}^{2m})/m\right\}^{1/8}.$$

Analysis showed that the expression $M(\bar{r})$ changes very little along the radius and in the range $0.7 < m < 1$ could take the value $M(\bar{r}) \approx 0.85$. Equation (4.2), with the boundary condition $r = 1$, $\mathrm{Re}\varphi^{**} = 0$, has the analytical solution

$$\mathrm{Re}_\varphi^{**} = \left[\frac{1{,}25A\,\mathrm{Re}_k}{N-m+0{,}75}\,\frac{(1-\bar{r})^{N-m+0{,}75}}{\bar{r}N}\right]^{0{,}8}, \tag{4.3}$$

$$N = 1{,}25\,[1-\bar{W}(1-m)],$$

$$A = B/2\bar{\delta}_m^{2n-1/4}\,(\bar{\delta}_m^{-2n}-1)\,M(\bar{r}) \simeq 0{,}1.$$

With the rotation of the fluid with constant circulation outside the boundary layers (m = 1), Eq. (4.3) is considerably simplified:

$$\mathrm{Re}_{\varphi.}^{**} = 0{,}03\frac{(1-\bar{r})^{0,8}}{\bar{r}}\mathrm{Re}_{k}^{0,8}. \tag{4.4}$$

A comparison of analytical expressions (4.3) and (4.4) with numerical solution of Eq. (4.1) using the Runge–Kutta method indicates good agreement. Further analysis of potential flow in the region outside the boundary layers is carried out for simplification and clarity.

The variation of $\mathrm{Re}_{\varphi}^{**}$ along the radius of the end wall is shown in Fig. 5 for the potential flow in the core ($\mathrm{Re}_k = 1.3\cdot10^5$). It is seen that computation based on Eq. (4.4) (line 1) describes the experiment [1, 2] well. Here it is necessary to keep in view that Eq. (4.4) is valid only for the developing region whose inner radius $\bar{r}^* \approx 0.6$ for the tests shown in Fig. 5, where line 2 is the computation for the developed flow region from Eq. (4.11).

An expression for the momentum thickness in the tangential direction is found from Eq. (4.4):

$$\delta_{\varphi}^{**} = 0{,}0475\frac{(1-\bar{r})^{0,3}}{(1+\bar{r})^{0,5}}\mathrm{Re}_{k}^{-0,2}R_k \tag{4.5}$$

and the data given in the table are used to find the thickness of the end-wall boundary layer:

$$\delta = 0{,}512\frac{(1-\bar{r})^{0,3}}{(1+\bar{r})^{0,5}}\mathrm{Re}_{k}^{-0,2}R_k. \tag{4.6}$$

According to expression (4.6), the thickness of the end-wall boundary layer depends weakly on Re_k and linearly increases with an increase in the radius of the chamber. Let us determine the volume flow of the gas convected in the radial direction by the boundary layer on one of the end walls. Using the expression for the integral parameter C,

$$Q_{\tau} = 2\pi r\int_0^{\delta} u\,dz = 2\pi\bar{r}C\,\mathrm{Re}_{\varphi}^{**}\mathrm{Re}_{k}^{-1}\Gamma_k R_k. \tag{4.7}$$

Taking into account Eq. (4.4) and putting C = 5.4 according to Table 1, we get

$$Q_{\tau} \simeq (1-\bar{r})^{0,8}\,\Gamma_k\,\mathrm{Re}_{k}^{-0,2}R_k. \tag{4.8}$$

Normalizing the flow through the end-wall boundary layer with respect to the entire fluid entering the chamber,

$$\bar{Q}_{\tau} = Q_{\tau}/Q_k = (1-\bar{r})^{0,8}\,\mathrm{Re}_{k}^{-0,2}\,\mathrm{Ro}^{-1}. \tag{4.9}$$

Here $\mathrm{Ro} = Q_k/\Gamma_k R_k$ is the Rossby number that characterizes the strength of the vortex rollup at the inlet to the vortex chamber.

Computed results for the variation of fluid flow along the radius of the chamber through the end-wall boundary layer are shown in Fig. 6. Computations using Eq. (4.9) (curve 1) and numerical results [1, 8] (curves 2 and 3, respectively) are in fairly close agreement; the deviation of experimental data [1-3] from computed results is explained by the fact that the flow in experiments is not potential.

Equation (4.9) is used to determine the radius $\bar{r}^*$ at which the entire fluid enters the boundary layer at the upper and lower end walls, i.e., $\bar{Q}_T = 0.5$:

$$\bar{r}^* = 1 - 0{,}42\,\mathrm{Re}^{0,25}\mathrm{Ro}^{1,25}. \tag{4.10}$$

Consider the developed flow region of the boundary layer ($\bar{r}_0 < \bar{r} < \bar{r}^*$), where the region outside the end-wall layers are noncirculation in the radial direction, i.e., $u_0 = 0$. It is possible to determine from (4.7) that $\mathrm{Re}_{\varphi}^{**}$ in this region is inversely proportional to the radius:

$$\mathrm{Re}_{\varphi}^{**} = \mathrm{Re}_k\,\mathrm{Ro}/4\pi C\bar{r} = 0{,}0147\,\mathrm{Re}_k\,\mathrm{Ro}/\bar{r}. \tag{4.11}$$

The nature of the variation of Reynolds number in regions I and II (see Fig. 1) is different because of the manner in which the boundary layers are formed in these regions.

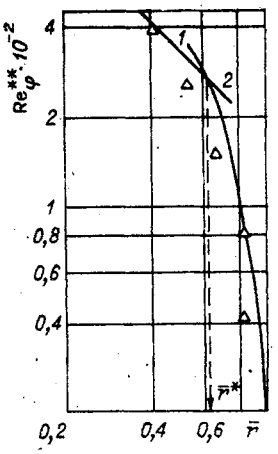

Fig. 5

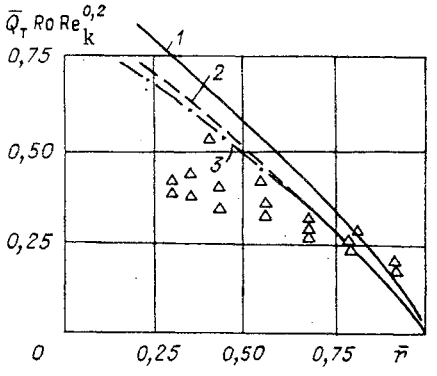

Fig. 6

The circulation distributions along the radius of the no-flow zone II, and also the distributions of radial velocities, boundary-layer thickness, and other characteristics are found from the simultaneous solution of Eqs. (1.5) and (4.11). Assuming that the circumferential velocity in this region follows the relation $v_0 \bar{r}^{m(\bar{r})} = 1$, from Eqs. (1.5) and (4.11) we get

$$\frac{dm}{d\bar{r}} \ln \bar{r} = \frac{1-m}{\bar{r}} - 0{,}5\,\bar{r}^{1,25-m}\left[1 + 0{,}69\left(1-\bar{r}^{2m}\right)/m\right]^{3/8} \times \\ \times \left[\left(1-\bar{r}^{2m}\right)/m\right]^{1/8} Re_k^{-0,25}\, Ro^{-1,25}. \tag{4.12}$$

The boundary condition is $m = 1$ at $\bar{r} = \bar{r}^*$. Equation (4.12) was numerically solved in the range of variation of the expression $Re_k^{0.25} Ro^{1.25} = 0.5\text{-}1.8$, that occurs in practical vortex setups. As a result of the numerical solution as a function of the radius of the chamber and its mass flux and geometric parameters, the exponential index is determined as

$$m = f\left(\bar{r},\, Re_k^{0,25}\, Ro^{1,25}\right). \tag{4.13}$$

Using Eqs. (4.13), (4.11), and (2.7), it is possible to compute all the required characteristics in the developed flow region.

Let us now analyze in detail the results obtained. It follows from Eq. (4.8) that the fluid flow Q_T through the end-wall boundary layer with fixed value of the current radius depends only on the circulation at the periphery of the chamber Γ_k and its radius. The chamber height H_k and flux Q_k through it at constant values of Γ_k and R_k do not have any influence on the boundary-layer characteristics. It is possible to come to such a conclusion by analyzing the studies [4-8], whose authors either do not emphasize this conclusion, which is important in our view, or assume [4, 5] that the chamber height has an influence on the flow in the boundary layers and, consequently, even outside them. Obviously, in practical situations, due to different contributions of the specifics of the formation of secondary circulating flows, from skin friction on the lateral surface to the coefficient of velocity conservation in chambers of various sizes, the chamber height will have some influence on the aerodynamics as a whole. However, in the present ideal-flow model, in which there is no loss of circumferential velocity at the periphery and secondary flows are absent, the nature of boundary-layer development is determined only by the radius of the chamber and the circumferential velocity at the periphery.

Equation (4.10) makes it possible to find the extent of the region I along the chamber radius. The vortex chamber is circulatory, i.e., when $\bar{r}^* < \bar{r}_0$, with

$$Re_k^{0,25}\, Ro \geq 2{,}38\left(1-\bar{r}_0\right). \tag{4.14}$$

We note that computations carried out in [8] gave results close to Eqs. (4.10) and (4.14). In [4], the author also comes to the conclusion that circulation distribution depends on the unique parameter

$$BLC^* = \frac{2fR_k v_k}{H_k u_k}\left(\frac{u_k H_k}{2\nu}\right)^{-1/4} = 0{,}5\,\mathrm{Re}_k^{-0,25}\,\mathrm{Ro}^{-1,25}, \qquad (4.15)$$

where f = 0.021 is the coefficient of friction at the end wall.

The critical parameter in [4, 8], as also in the present study, is $\mathrm{Re}_k^{0.25}\mathrm{Ro}^{1.25}$. Here Ro characterizes the geometry of the vortex chamber resulting in the moment of momentum at the periphery of the chamber, and does not depend on the length of the chamber:

$$\mathrm{Ro} = \frac{Q_k}{\Gamma_k R_k} = \frac{F_{in} v_{in}}{v_{in}\cos\beta R_k^2} = \frac{F_{in}}{R_k^2\cos\beta}.$$

here F_{in} is the area of inlet slots, and β is the angle of inclination of these slots to the tangential direction. If Eq. (4.11) is expressed in the form

$$\bar{r}^* = 1 - \frac{0{,}42}{\nu^{0,25}}\frac{1}{\Gamma_k}\left(\frac{Q_k}{R_k}\right)^{1,25},$$

then it is clear that an increase in circulation at the periphery or a reduction in the fluid flow through the chamber leads to a shortening of the developing region and a larger segment of the chamber becomes a dead air region. In the limiting case ($\Gamma_k \to \infty$ or $Q_k \to 0$), $\bar{r}^* \to 1$ and the entire mass flow, starting from the periphery of the chamber, passes through boundary layers; and when $\Gamma_k \to 0$ or $Q_k \to \infty$, transition to developed flow is not observed.

Thus, the above analysis showed that the criterion that determines the strength of the turbulent end-wall layer in the vortex chamber is the expression $\mathrm{Re}_k^{0.25}\mathrm{Ro}^{1.25}$; when $\mathrm{Re}_k^{0.25}\cdot\mathrm{Ro}^{1.25} > 2.38(1 - \bar{r}_0)$ for the potential flow, the vortex chamber is circulatory in the radial direction within its entire volume.

LITERATURE CITED

1. T. J. Kotas, "Turbulent boundary-layer flow on the end wall of a cylindrical vortex chamber," Heat and Fluid Flow, 5, No. 2 (1975).
2. T. J. Kotas, "An experimental study of the three-dimensional boundary layer on the end wall of a vortex chamber," Proc. R. Soc., 352, No. 1669, London (1976).
3. V. I. Bagryantsev, É. P. Volchkov, V. I. Terekhov, et al., "Investigation of flow in vortex chamber using laser-Doppler anemometry," Preprint, Inst. Teplo Fiziki, Siberian Branch, Academy of Sciences of the USSR (1980).
4. D. N. Wormley, "An analytical model for the incompressible flow in short vortex chambers," Trans. ASME, Ser. D, 91, No. 2 (1969).
5. M. A. Gol'dshtik, Vortex Flows [in Russian], Nauka, Novosibirsk (1981).
6. M. L. Rosenzweig, W. S. Lewellen, and D. N. Ross, "Confined vortex flows with boundary-layer interaction," AIAA J., No. 12 (1964).
7. N. Rott and W. Lewellen, "Boundary layers and their interactions in rotating flows," Progr. Aeronaut. Sci., 7 (1975).
8. E. P. Sukhovich, "Aerodynamics of vortex chamber," Izv. Akad. Nauk Latvian SSR, Ser. Fiz. Tekh. Nauk, No. 4 (1969).
9. É. P. Volchkov, Fluid Wall Curtain [in Russian], Nauka, Novosibirsk (1983).
10. É. P. Volchkov, S. V. Semenov, and V. I. Terekhov, "End-wall boundary layer in vortex chamber," in: The Structure of Forced and Thermogravitational Flows [in Russian], Inst. of Thermal Physics, Siberian Branch, Academy of Sciences of the USSR, Novosibirsk (1983).
11. É. P. Volchkov and I. I. Smul'skii, "Aerodynamics of vortex chamber with suction through lateral surface," Preprint 38-79, Inst. Thermal Physics, Siberian Branch, Academy of Sciences of the USSR (1979).
12. É. P. Volchkov, V. I. Kislykh, and I. I. Smul'skii, "Experimental study of the aerodynamics of vortex chamber with end-wall suction," in: The Structure of Wall Boundary Layer [in Russian], Inst. Thermal Physics, Siberian Branch, Academy of Sciences of the USSR, Novosibirsk (1978).
13. H. Schlichting, Boundary-Layer Theory, McGraw-Hill, New York (1968).
14. S. S. Kutateladze and A. I. Leont'ev, Heat and Mass Transfer and Skin Friction in Turbulent Boundary Layer [in Russian], Energiya, Moscow (1972).
15. G. I. Abramovich, Theory of Turbulent Jets [in Russian], Fizmatgiz, Moscow (1960).